

New layered fluorosulfide SrFBiS₂

Hechang Lei, Kefeng Wang, Milinda Abeykoon, Emil S. Bozin, and C. Petrovic
*Condensed Matter Physics and Materials Science Department,
Brookhaven National Laboratory, Upton, NY 11973, USA*
(Dated: September 5, 2018)

We have synthesized a new layered BiS₂-based compound SrFBiS₂. This compound has similar structure to BiS₂. It is built up by stacking up SrF layers and NaCl-type BiS₂ layers alternatively along the c axis. Electric transport measurement indicates that SrFBiS₂ is a semiconductor. Thermal transport measurement shows that SrFBiS₂ has a small thermal conductivity and large Seebeck coefficient. First principle calculations are in agreement with experimental results and show that SrFBiS₂ is very similar to LaOBiS₂ which becomes superconductor with F doping. Therefore, SrFBiS₂ may be a parent compound of new superconductors.

I. INTRODUCTION

Low-dimensional superconductors with layered structure have been extensively studied and still attract much interest due to their exotic superconducting properties and mechanism when compared to conventional BCS superconductors. The examples include high T_c cuprates,¹ Sr₂RuO₄,² Na_xCoO₂·H₂O,³ and iron-based superconductors.⁴ The discovery of LnOFePn (Ln = rare earth elements, Pn = P, As) in particular revitalises the study of layered compounds with mixed anions, paving a way to materials with novel physical properties. For example, Ln₂O₂TM₂OCh₂ (TM = transition metals, Ch = S, Se) show strong electron-electron interactions and Mott insulating state on the two dimensional (2D) frustrated antiferromagnetic (AFM) checkerboard spin-lattice.^{5–9} Very recently, bulk superconductivity was found in BiS₂-type layered compounds with mixed anions: Bi₄O₄S₃ and Ln(O,F)BiS₂.^{10–12} Experimental and theoretical studies indicate that these materials exhibit multiband behaviors with dominant electron carriers originating from the Bi 6p_x and 6p_y bands in the normal state.^{13–16} On the other hand, compounds with mixed anions exhibit remarkable flexibility of structure. Different two-dimensional (2D) building blocks, such as [LnO]⁺, [AEF]⁺ (AE = Ca, Sr, Ba), [Ti₂OPn₂]²⁻, [FePn]⁻, and [TM₂OCh₂]²⁻, can sometimes be integrated to form new materials.^{4,17–21} Individual building blocks often keep their structural and electronic properties after being combined together.¹⁹

In this work, we report the discovery of a new BiS₂-based layered compound SrFBiS₂. It contains NaCl-type BiS₂ layer and shows semiconducting behavior with relatively large thermopower. Theoretical calculation indicates that this compound is very similar to LaOBiS₂.

II. EXPERIMENT

A. Synthesis.

SrFBiS₂ polycrystals were synthesized by a two-step solids state reaction. First, Bi₂S₃ was prereacted by re-

acting Bi needles (purity 99.99%, Alfa Aesar) with sulfur flakes (purity 99.99%, Aldrich) in an evacuated quartz tube at 600 °C for 10 h. Then Bi₂S₃ was mixed with stoichiometric SrF₂ (purity 99%, Alfa Aesar) and SrS (purity 99.9%, Alfa Aesar) and intimately ground together using an agate pestle and mortar. The ground powder was pressed into 10 mm diameter pellets. We used a maximum pressure of 5 tons. The pressed pellet was loaded in an alumina crucible and then sealed in quartz tubes with Ar under the pressure of 0.15 atmosphere. The quartz tubes were heated up to 600 °C in 10 h and kept at 600 °C for another 10 h.

B. Structure and Composition Analysis.

Phase identity and purity were confirmed by powder X-ray diffraction carried out by a Rigaku Miniflex X-ray machine with Cu K_α radiation ($\lambda = 1.5418 \text{ \AA}$). Structural refinement of powder SrFBiS₂ sample was carried out by using Rietica software.²² Synchrotron X-ray experiment was conducted at 300 K on X17A beamline of the National Synchrotron Light Source (NSLS) at Brookhaven National Laboratory (BNL). The setup utilized X-ray beam 0.5 mm × 0.5 mm in size and $\lambda = 0.1839 \text{ \AA}$ ($E = 67.4959 \text{ keV}$), conditioned by two-axis focusing with one-bounce sagittally-bent Laue crystal monochromator, and Perkin-Elmer image plate detector mounted perpendicular to the primary beam path. Finely pulverized sample packed in cylindrical polyimide capillary 1mm in diameter was placed 204 mm away from the detector. Multiple scans were performed to a total exposure time of 120 s. The 2D diffraction data were integrated and converted to intensity versus 2θ using the software FIT2D.²³ The intensity data were corrected and normalized and converted to atomic pair distribution function (PDF), $G(r)$, using the program PDFgetX2.²⁴ The average stoichiometry of SrFBiS₂ polycrystal was determined by examination of multiple points using an energy-dispersive x-ray spectroscopy (EDX) in a JEOL JSM-6500 scanning electron microscope.

C. Electrical and Thermal Transport Measurements.

The sample pellets were cut into rectangular bar and the surface is polished by sandpaper. Thin Pt wires were attached using silver epoxy for four probe resistivity measurements. Electrical and thermal transport measurements were carried out in Quantum Design Physical Property Measurement System (PPMS-9).

D. Band Structure Calculations.

First principle electronic structure calculation were performed using experimental crystallographic parameters within the full-potential linearized augmented plane wave (LAPW) method²⁵ implemented in WIEN2k package.²⁶ The general gradient approximation (GGA) of Perdew *et al.*,²⁷ was used for exchange-correlation potential. The LAPW sphere radius were set to 2.5 Bohr for all atoms, and the converged basis corresponding to $R_{min}k_{max} = 7$ with additional local orbital were used where R_{min} is the minimum LAPW sphere radius and k_{max} is the plane wave cutoff.

III. RESULTS AND DISCUSSION

A. Structure and Compostion.

Fig. 1(a) shows the powder XRD pattern of SrFBiS₂ measured by Rigaku Miniflex. Almost all of reflections can be indexed using the P4/nmm space group. The unidentified peaks belong to the second phase of Bi₂S₃. Using two-phase Le Bail fitting, the refined lattice parameters of SrFBiS₂ are $a = 4.084(2)$ Å and $c = 13.798(2)$ Å. When compared to LaOBiS₂, the a-axial lattice parameter is larger and the c-axial one is slightly smaller.¹¹ The PDF structural analysis was carried out using the program PDFgui.²⁸ The SrFBiS₂ data are explained well within the model having P4/nmm symmetry with $a = 4.079(2)$ Å and $c = 13.814(5)$ Å ($R_{wp} = 0.138$, $\chi^2 = 0.024$). It is consistent with the fitting results obtained from Miniflex. The final fit is shown in Fig. 1(b), and the results are summarized in Table 1. In addition to the principal phase, the sample is found to have $\sim 16(1)$ wt% of Bi₂S₃ impurity with Pnma symmetry, which is also observed in Fig. 1(a). Structure of SrFBiS₂ is similar to LaOBiS₂, which is built up by stacking the rock-salt-type Bi₂S₃ layer and fluorite-type SrF layer alternatively along the c axis as shown Fig. 1(c). The EDX spectrum of polycrystal confirms the presence of Sr, F, Bi, and S. The average atomic ratios determined from EDX are Sr : F : Bi : S = 1.00(4) : 1.00(9) : 1.03(5) : 1.88(4) when setting the content of Sr as 1. It confirms the formula of obtained compound is SrFBiS₂.

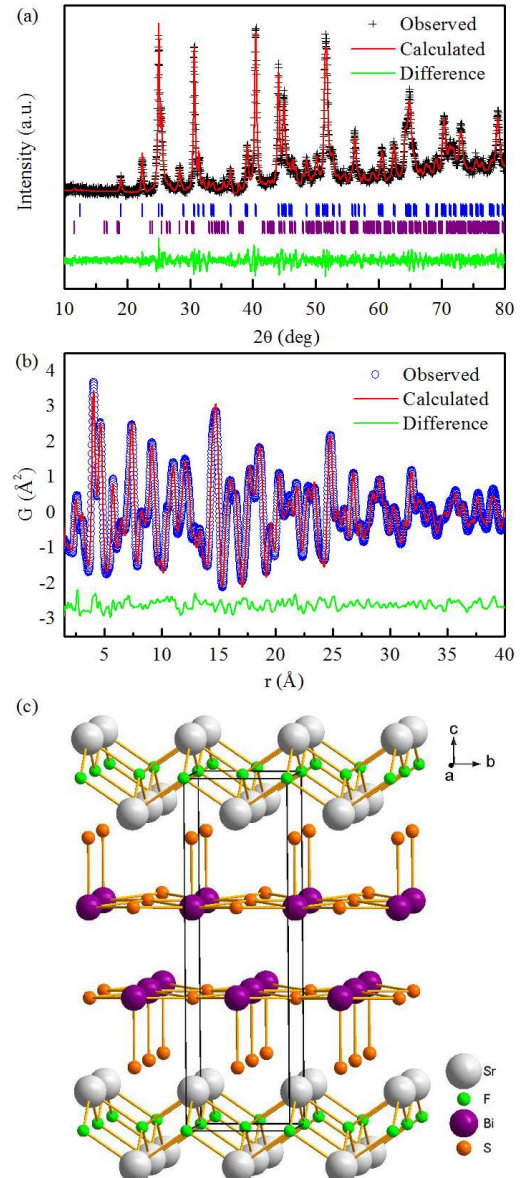


FIG. 1. (a) Powder XRD pattern of SrFBiS₂ and the fitted result using two-phase Le Bail fitting. Crosses are experimental data, red line is fitted spectra, green line is the difference between experimental data and fitted spectra, vertical lines are calculated Bragg-positions for SrFBiS₂ (upper) and Bi₂S₃ (lower), respectively. (b) Synchrotron PDF refinement of data taken at room temperature. (c) Crystal structure of SrFBiS₂. The biggest white, big purple, medium orange, and small green balls represent Sr, Bi, S, and F ions, respectively.

B. Electrical Properties.

As shown in Fig. 2, the resistivity $\rho(T)$ of SrFBiS₂ polycrystalline shows a semiconducting behavior in the measured temperature region (1.9–300 K). It should be noted that Bi₂S₃ polycrystal shows metallic behavior because of sulfur deficiency.²⁹ The impurity may have some minor influence on the absolute value of resis-

TABLE I. Crystallographic Data for SrFBiS₂ obtained from synchrotron powder XRD.

Chemical Formula	SrFBiS ₂		
Formula Mass (g/mol)	379.73		
Crystal System	Tetragonal		
Space Group	P4/nmm (No. 129)		
<i>a</i> (Å)	4.079(2)		
<i>c</i> (Å)	13.814(5)		
<i>V</i> (Å ³)	229.8(3)		
<i>Z</i>	2		
Density (g/cm ³)	5.51		
Atom site	x	y	<i>U_{eq}</i> (Å ²) ^a
Sr	2c	1/4	0.0069(4)
F	2a	3/4	0.033(2)
Bi	2c	1/4	0.0183(3)
S1	2c	1/4	0.060(2)
S2	2c	1/4	0.019(1)

^a *U_{eq}* is defined as one-third of the orthogonalized *U_{ij}* tensor.

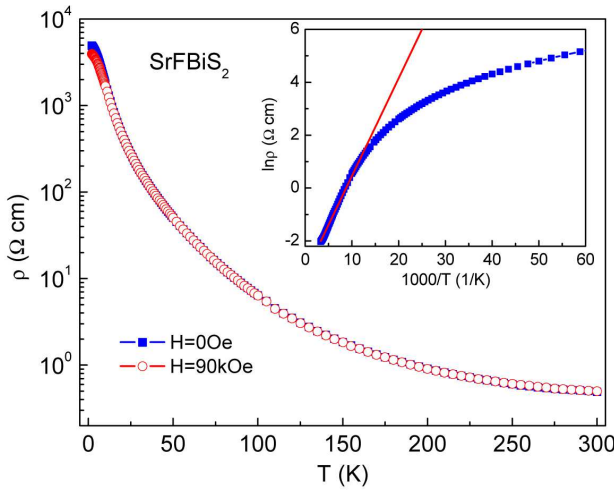


FIG. 2. Temperature dependence of the resistivity $\rho(T)$ of the SrFBiS₂ at $H = 0$ (closed blue square) and 90 kOe (open red circle). Inset shows the fitted result using thermal activation model for $\rho(T)$ at zero field where the red line is the fitting curve.

tivity, but the semiconducting behavior should be intrinsic. Neglecting the grain boundary contribution, the room-temperature resistivity $\rho(300 \text{ K})$ is about 0.5 Ω·cm. Using the thermal activation model $\rho_{ab}(T) = \rho_0 \exp(E_a/k_B T)$ (ρ_0 is a prefactor, E_a thermal activated energy and k_B the Boltzmann's constant) to fit the $\rho(T)$ at high temperature (75 K - 300 K) (inset of Fig. 2), we obtain $E_a = 31.8(3)$ meV. The semiconductor behavior is consistent with theoretical calculation result shown below. On the other hand, theoretical calculations have indicated that undoped LaOBiS₂ is also a

semiconductor, which is partially consistent with the experimental result.^{13,30} Transport measurement indicates that LaOBiS₂ shows semiconducting behavior at $T < 200$ K, but exhibit an upturn of resistivity at higher temperature. The origin of the upturn is unclear. Therefore, the replacement of LaO by SrF should not change the band structure and thus physical properties too much, especially at low temperature, similar to the relation between SrFeAs and LaOFeAs.^{18,31} The slight differences between LaOBiS₂ and SrFBiS₂, such as larger *a*-axial and smaller *c*-axial lattice parameters, could result in changing of physical properties at higher temperature. Note that the semiconducting $\rho(T)$ in LaOBiS₂ and SrFBiS₂ are different from those in parent compounds of iron pnictide superconductors. The latter show metallic behaviors at high temperature and semiconducting-like upturn in resistivity curve related to the spin density wave (SDW) transition. There is no significant magnetoresistance in SrFBiS₂ up to 90 kOe magnetic field.

C. Thermal Transport Properties.

The temperature dependences of the thermal conductivity $\kappa(T)$ and thermoelectric power (TEP) $S(T)$ for SrFBiS₂ in zero field between 2 and 350 K are shown in Fig. 3. The electronic thermal conductivity $\kappa_e(T)$ estimated from the Wiedemann-Franz law using a value for the Lorenz number of $2.44 \times 10^{-8} \text{ W } \Omega/\text{K}^2$ was less than 5×10^{-6} of $\kappa(T)$. Therefore, lattice thermal conductivity dominates $\kappa_L(T)$ which exhibits a peak at around 60 K (Fig. 1(a)). The peak in $\kappa(T)$ commonly arises since different phonon scattering processes usually dominate in different temperature ranges. Umklapp scattering dominates at high temperatures, while boundary and point-defect scattering dominate at low and intermediate tem-

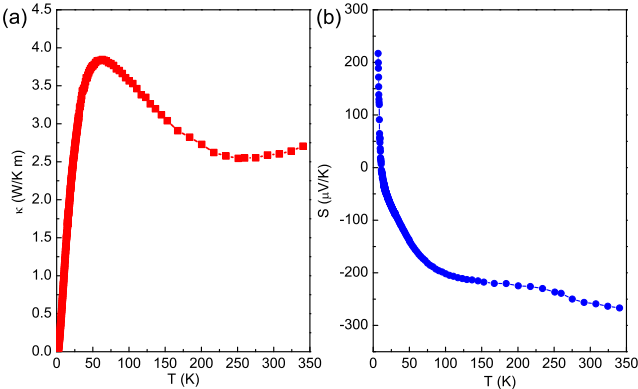


FIG. 3. Temperature dependence of (a) thermal conductivity and (b) thermoelectric power for SrFBiS_2 under zero magnetic field within a temperature range from 2 to 340 K.

peratures, respectively.³² On the other hand, the $\kappa(T)$ of SrFBiS_2 shows similar behavior to $\text{Bi}_4\text{O}_4\text{S}_3$ but with different peak position and absolute value.¹⁶ For TEP $S(T)$ of SrFBiS_2 , there is a reversal in sign at about 11 K, i.e., hole-like carrier changes into electron-like carrier which is dominant at room temperature. According to two band model, $S = |S_h|\sigma_h - |S_e|\sigma_e/(\sigma_e + \sigma_h)$.¹⁶ If we assume that S_h and S_e are temperature independent, it suggests that electron and hole conductivities change dramatically with temperature: at low temperature, $\sigma_h > \sigma_e$ whereas $\sigma_e > \sigma_h$ above 11 K. Hole-like carrier may originate from defect induced p-type doping. With increasing temperature, electron-like carrier due to intrinsic band excitation increase significantly, finally leading to $\sigma_e > \sigma_h$ and a sign change in $S(T)$. Similar behavior was observed in LaOZnP and p-type Si.^{33,34} Even though the $S(T)$ in SrFBiS_2 is significant and not much smaller than in classics thermoelectric materials,³⁵ its low electrical conductivity makes its figure of merit ZT ($ZT = \sigma S^2 T / \kappa$) extremely small.

D. Electronic Structure.

First principle calculations (Fig. 4) confirm that SrFBiS_2 is a semiconductor with a direct band gap of 0.8 eV located at X point. This is similar to LaOBiS_2 where the energy gap was found to be 0.82 eV.³⁶ The calculation confirms the results of transport measurement. Similar to LaOBiS_2 ,^{13,36} both S 3p and Bi 6p states are located around the Fermi level (-2.0 to 2.0 eV) in SrFBiS_2 . Thus there is a strong hybridization between S 3p and Bi 6p states. The absence of dispersion along $\Gamma - Z$ line suggests quasi two dimensional character of the band structure in SrFBiS_2 (Fig. 4(b)). In LaOBiS_2 , F doping results in metallic states and superconductivity at low temperature. Main influence of F substitution is a carrier doping that shifts the Fermi level and has only minor effect on the lowest conduction band. Due to similarity between SrFBiS_2 and LaOBiS_2 , new supercon-

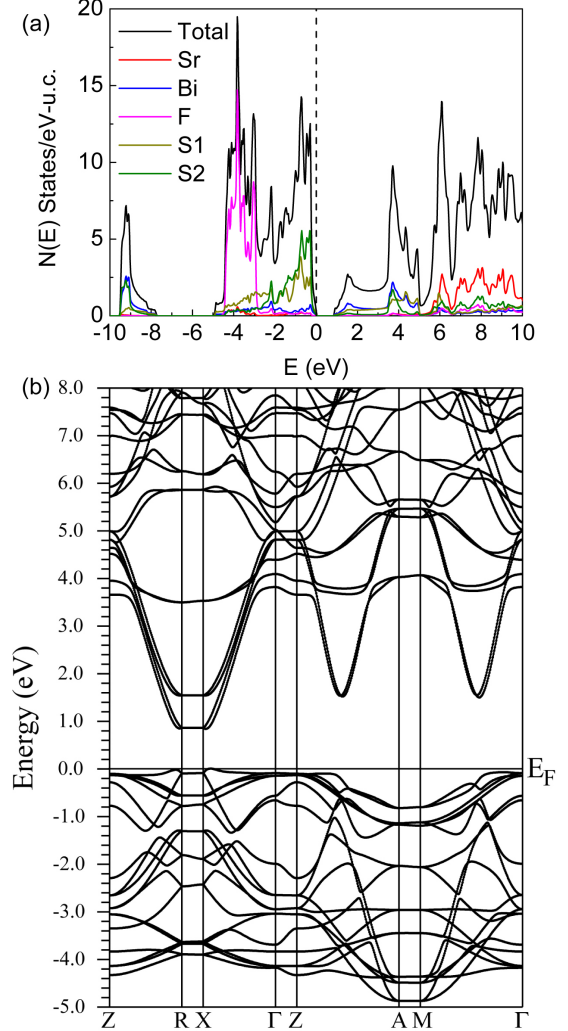


FIG. 4. (a) Total and atom resolved density of states and (b) band structure of SrFBiS_2 .

ductors could be obtained by chemical substitution.

IV. CONCLUSION

In summary, we report a discovery of a new layered fluorosulfide SrFBiS_2 . It contains NaCl-type BiS_2 layer similar to $\text{Bi}_4\text{O}_4\text{S}_3$ and $\text{Ln(O,F)}\text{BiS}_2$ superconductors. SrFBiS_2 polycrystals shows semiconducting behavior between 2 K and 300 K. We observe rather small thermal conductivity and large TEP with sign reversal at low temperature. Theoretical calculation confirms the semiconducting behavior and indicates similar DOS and band structure to undoped LaOBiS_2 . Because of the similarity between SrFBiS_2 and the parent compound of BiS_2 -based superconductors, it is of interest to investigate the doping effects on physical properties of SrFBiS_2 . It could pave a way to new members in this emerging family of

BiS₂-based superconductors.

V. ACKNOWLEDGEMENTS

We thank John Warren for help with SEM measurements. Work at Brookhaven is supported by the U.S. DOE under Contract No. DE-AC02-98CH10886 and

in part by the Center for Emergent Superconductivity, an Energy Frontier Research Center funded by the U.S. DOE, Office for Basic Energy Science (H. L. and C. P.). This work benefited from usage of X17A beamline of the National Synchrotron Light Source at Brookhaven National Laboratory. We gratefully acknowledge Zhong Zhong and Jonathan Hanson for their help with the X17A experiment setup.

-
- ¹ J. G. Bednorz and K. A. Muller, *Z. Physik B* **64**, 189 (1986).
- ² Y. Maeno, H. Hashimoto, K. Yoshida, S. Nishizaki, T. Fujita, J. G. Bednorz, and F. Lichtenberg, *Nature* **372**, 532 (1994).
- ³ K. Takada, H. Sakurai, E. Takayama-Muromachi, F. Izumi, R. A. Dilanian, and T. Sasaki, *Nature* **422**, 53 (2003).
- ⁴ Y. Kamihara, T. Watanabe, M. Hirano, and H. Hosono, *J. Am. Chem. Soc.* **130**, 3296 (2008).
- ⁵ J. M. Mayer, L. F. Schneemeyer, T. Siegrist, J. V. Waszczak and B. Van Dover, *Angew. Chem., Int. Ed. Engl.* **31**, 1645 (1992).
- ⁶ C. Wang, M. Q. Tan, C. M. Feng, Z. F. Ma, S. Jiang, Z. A. Xu, G. H. Cao, K. Matsubayashi and Y. Uwatoko, *J. Am. Chem. Soc.* **132**, 7069 (2010).
- ⁷ J.-X. Zhu, R. Yu, H. Wang, L. L. Zhao, M. D. Jones, J. Dai, E. Abrahams, E. Morosan, M. Fang and Q. Si, *Phys. Rev. Lett.* **104**, 216405 (2010).
- ⁸ N. Ni, E. Climent-Pascual, S. Jia, Q. Huang and R. J. Cava, *Phys. Rev. B* **82**, 214419 (2010).
- ⁹ D. G. Free, N. D. Withers, P. J. Hickey and J. O. Evans, *Chem. Mater.* **23**, 1625 (2011).
- ¹⁰ Y. Mizuguchi, H. Fujihisa, Y. Gotoh, K. Suzuki, H. Usui, K. Kuroki, S. Demura, Y. Takano, H. Izawa, O. Miura, *Phys. Rev. B* **86**, 220510(R) (2012).
- ¹¹ Y. Mizuguchi, S. Demura, K. Deguchi, Y. Takano, H. Fujihisa, Y. Gotoh, H. Izawa, O. Miura, *J. Phys. Soc. Jpn.* **81**, 114725 (2012).
- ¹² S. Demura, Y. Mizuguchi, K. Deguchi, H. Okazaki, H. Hara, T. Watanabe, S. J. Denholme, M. Fujioka, T. Ozaki, H. Fujihisa, Y. Gotoh, O. Miura, T. Yamaguchi, H. Takeya, and Y. Takano, arXiv 1207.5248.
- ¹³ H. Usui, K. Suzuki, K. Kuroki, *Phys. Rev. B* **86**, 220501(R) (2012).
- ¹⁴ S. Li, H. Yang, J. Tao, X. Ding, and H.-H. Wen, arXiv 1207.4955.
- ¹⁵ S. K. Singh, A. Kumar, B. Gahtori, Shruti, G. Sharma, S. Patnaik, and V. P. S. Awana, *J. Am. Chem. Soc.* **134**, 16504 (2012).
- ¹⁶ S. G. Tan, L. J. Li, Y. Liu, P. Tong, B. C. Zhao, W. J. Lu, Y. P. Sun, *Physica C* **483**, 94 (2012).
- ¹⁷ S. Matsuishi, Y. Inoue, T. Nomura, H. Yanagi, M. Hirano, and H. Hosono, *J. Am. Chem. Soc.* **130**, 14428 (2008).
- ¹⁸ F. Han, X. Y. Zhu, G. Mu, P. Cheng, and H.-H. Wen, *Phys. Rev. B* **78**, 180503 (2008).
- ¹⁹ H. Kabbour, L. Cario, and F. Boucher, *J. Mater. Chem.* **15**, 3525 (2005).
- ²⁰ R. H. Liu, J. S. Zhang, P. Cheng, X. G. Luo, J. J. Ying, Y. J. Yan, M. Zhang, A. F. Wang, Z. J. Xiang, G. J. Ye and X. H. Chen, *Phys. Rev. B* **83**, 174450 (2011).
- ²¹ R. H. Liu, Y. A. Song, Q. J. Li, J. J. Ying, Y. J. Yan, Y. He, and X. H. Chen, *Chem. Mater.* **22**, 1503 (2010).
- ²² Hunter B. (1998) "Rietica - A visual Rietveld program", International Union of Crystallography Commission on Powder Diffraction Newsletter No. 20, (Summer) <http://www.rietica.org>
- ²³ A. P. Hammersley, S.O. Svenson, M. Hanfland, and D. Hauserman, *High Press. Res.* **14**, 235 (1996).
- ²⁴ X. Qiu, J. W. Thompson, and S. J. L. Billinge, *J. Appl. Crystallogr.* **37**, 678 (2004).
- ²⁵ M. Weinert, E. Wimmer, and A. J. Freeman, *Phys. Rev. B* **26**, 4571 (1982).
- ²⁶ P. Blaha, K. Schwarz, G. K. H. Madsen, D. Kvasnicka and J. Luitz, WIEN2k, An Augmented Plane Wave + Local Orbitals Program for Calculating Crystal Properties (Karlheinz Schwarz, Techn. Universität Wien, Austria), 2001. ISBN 3-9501031-1-2
- ²⁷ J. P. Perdew, K. Burke and M. Ernzerhof, *Phys. Rev. Lett.* **77**, 3865 (1996).
- ²⁸ C. L. Farrow, P. Juhas, J. W. Liu, D. Bryndin, E. S. Bozin, J. Bloch, Th. Proffen, and S. J. L. Billinge, *J. Phys.: Condens. Mater.* **19**, 335219 (2007).
- ²⁹ B. Chen, C. Uher, L. Iordanidis, and M. G. Kanatzidis, *Chem. Mater.* **9**, 1655 (1997).
- ³⁰ V. P. S. Awana, A. Kumar, R. Jha, S. Kumar, J. Kumar, and A. Pal, arXiv 1207.6845.
- ³¹ J. Dong, H. J. Zhang, G. Xu, Z. Li, G. Li, W. Z. Hu, D. Wu, G. F. Chen, X. Dai, J. L. Luo, Z. Fang, and N. L. Wang, *EPL* **83**, 27006 (2008).
- ³² J. Yang, D. T. Morelli, G. P. Meisner, W. Chen, J. S. Dyck, and C. Uher, *Phys. Rev. B* **65**, 094115 (2002).
- ³³ K. Seeger, in *Semiconductor Physics: An Introduction*, Springer-Verlag, Berlin (2004).
- ³⁴ K. Kayanuma, H. Hiramatsu, M. Hirano, R. Kawamura, H. Yanagi, T. Kamiya, and H. Hosono, *Phys. Rev. B* **76**, 195325 (2007).
- ³⁵ D. M. Rowe, in *Thermoelectrics Handbook: Macro to Nano*, Taylor & Francis, London (2006).
- ³⁶ X. Wan, H.-C. Ding, S. Y. Savrasov, and C.-G. Duan, arXiv 1208.1807.